Fluent simulation of a beta Stirling engine for very low temperatures

J.A. Auñón Hidalgo [a, * [0000-0002-2035-9366]], D. Núñez Gevorkian [b, [0000-0002-3581-7833]]

[a] *Department of Mechanical, Thermal and Fluid Engineering. Industrial Engineering School. University of Malaga, Malaga (29071), Spain. aunon@uma.es*

[b] *Department of Mechanical, Thermal and Fluid Engineering. Industrial Engineering School. University of Malaga, Malaga (29071), Spain. danigevorkian@uma.es*

Topics: *Stirling refrigerators and cryocoolers.*

Keyword: *ZIFF-1000 Stirling Engine, ANSYS-Fluent Simulation, thermodynamic analysis, heat transfer and fluid dynamics and energy efficiency and optimization.*

Abstract

This research article presents an in-depth study of the ZIFF-1000 Stirling engine, focusing on its simulation through ANSYS-Fluent software. The research initiates with a thorough study of the ZIFF-1000 engine, including its unique design features such as the crankshaft mechanism, simplified geometry, and the regenerator, along with the hot and cold heat exchangers. The work emphasizes the significance of these components in enhancing the engine's efficiency and operational reliability.

The main contribution of this study is the advanced simulation of the Stirling engine using ANSYS-Fluent for very low temperatures. This involved intricate processes like the adaptation of the engine's geometry for simulation, meticulous meshing, defining fluid and solid zones, and establishing dynamic meshing and boundary conditions. These simulations aimed to provide a comprehensive understanding of the engine's thermodynamic behavior and performance under various conditions.

The research highlights the simulation's capability to accurately predict the engine's performance, particularly focusing on aspects such as heat transfer, fluid flow dynamics, and energy efficiency. The simulation results are meticulously analyzed, providing critical insights into the engine's operational characteristics, such as temperature distribution, pressure fluctuations, and efficiency under different operating scenarios.

Moreover, the research discusses the challenges encountered during the simulation process, including the complexities associated with accurately replicating the physical phenomena within the engine and the limitations of the simulation tools.

In conclusion, this study not only advances the understanding of Stirling engine simulations but also proposes improvements for future research and practical applications of these engines in various industrial and environmental contexts. The findings of this research have significant implications for the design and optimization of Stirling engines, contributing to the development of more efficient and environmentally friendly energy systems.

Introduction

This research delves into the simulation of the ZIFF-1000 Stirling engine, a beta-type engine designed for cryogenic applications (**Figure 1**). Triggered by the University of Málaga's acquisition of this innovative machine, our aim is to contribute to the body of knowledge on cryogenic machinery and its technologies.

This research offers a detailed simulation of the ZIFF-1000 Stirling engine, a Soviet-manufactured beta-type engine designed for air liquefaction. This engine, based on Philips-developed technology, was created to bypass Philips patents, and achieve superior

**Corresponding author. E-mail address aunon@uma.es*

performance. Its modern counterparts are available from the Dutch company "Stirling Cryogenics BV," specifically the SPC-1 cryo-generator, with some parts being interchangeable with the ZIFF-1000. Before operation, the machine is charged with helium, the working fluid, which will increase in pressure as the engine runs. The cooling circuit is fed with ambient temperature water, which warms up by absorbing the heat removed from the air and the heat generated by the engine's moving parts.

The ZIFF-1000 operates on a Stirling cycle [3] executed by a compressor piston and a displacer piston, driven by a crankshaft using a crank-slider mechanism with a 110° phase shift between pistons to mimic the Stirling cycle's sequential volume changes. The engine's upper part, known as the liquefier, is an isolated volume connected to the thermodynamic cycle through a copper heat exchanger and a column that increases the heat exchange surface with the air to be liquefied. The engine also features a metallic mesh that collects moisture from the air, which freezes and blocks air passage through an upper opening—however, more liquid air generation occurs with this opening left open.

This study focuses on simulating the ZIFF-1000 engine's operation, incorporating its complex geometry, dynamic movement of pistons, and thermal interactions within the engine. By exploring the simplified but accurate representation of the engine's geometry and dynamics, the research aims to contribute to optimizing Stirling engines for cryogenic applications. This involves examining the engine's regenerator, cold and hot focus heat exchangers, and the effects of these components on the engine's efficiency and performance. Through this simulation, we intend to provide insights into improving cryogenic machinery's design and operational strategies, enhancing their application in industrial and environmental settings.

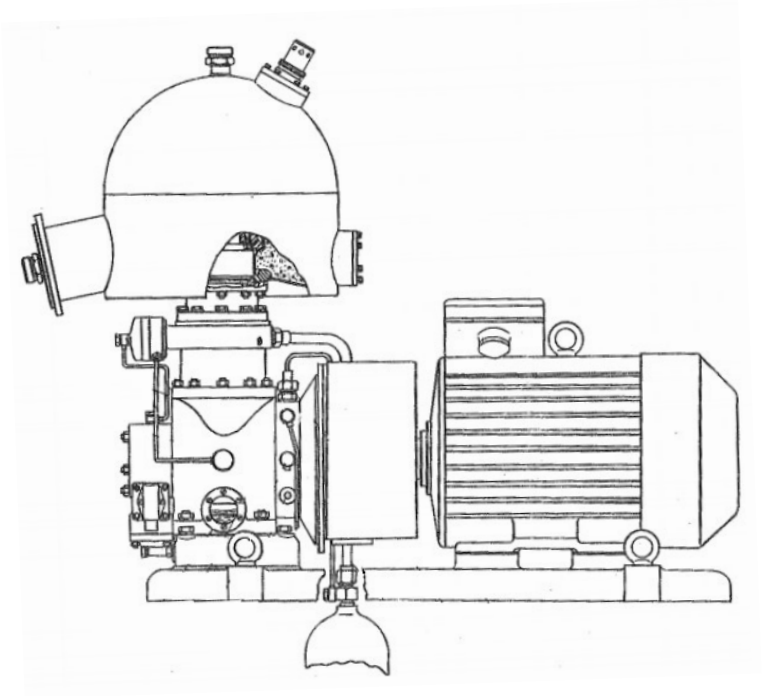

Figure 1. ZIF-100 machine representation.

Literature Review

The Stirling engine, recognized for its unique closed-loop regenerative cycle, adapts to a wide array of heat sources, offering a versatile and sustainable energy solution [1]. Originating in the 19th century by Robert Stirling as a safer alternative to the hazardous steam engines of the time [2], its design and efficiency have significantly evolved, benefiting from advancements in materials science and computational technologies. This evolution enables the engine to exploit diverse energy sources, including renewables like solar and geothermal power [3], making it suitable for a variety of applications from low-temperature

operations to power generation in isolated or sensitive environments. Recent studies have aimed at boosting the engine's performance by optimizing its design, selecting superior materials, and incorporating sophisticated regenerative components, with Computational Fluid Dynamics (CFD) simulations providing crucial insights into improving thermodynamic processes and design features [4][5][6][7][8]. Nonetheless, research continues to explore the potential of novel materials for key components like the regenerator and heat exchangers to further enhance the engine's efficiency, especially in low-temperature contexts [9].

ZIFF-1000 Stirling engine description and geometry creation.

The ZIFF-1000 Stirling engine represents a beta-type engine distinguished by its cryogenic functionality. Central to its operation is the helium gas acting as the working fluid, facilitating the refrigeration cycle pivotal to the engine's cryogenic application. The design features a sophisticated crankshaft mechanism that orchestrates the movement of the pistons, thereby driving the cycle.

The motion of the system has been modeled using the crank-slider mechanism (see **Figure 2**). This motion is employed for contouring, dynamic mesh configuration, and the selection of the time step to be followed.

The geometry to be modeled is complex due to the oil circuits, helium loading, and asymmetrical shapes of the moving parts and machine contours. Therefore, a simpler geometry has been represented while maintaining the volumes of the real geometry (see **Figure 3**).

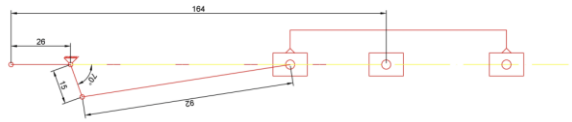

Figure 2. Kinematic diagram, with dimensions, of the crank-slider mechanism

Figure 3. Comparison of simplified geometry (green) with real geometry (blue)

The formula for velocity is as follows:

$$v = r \cdot \omega \cdot \left[-\sin(\theta + \omega \cdot t) - \frac{r \cdot \sin(2 \cdot (\theta + \omega \cdot t))}{2 \cdot \sqrt{l^2 - r^2 \cdot \cos^2(\theta + \omega \cdot t)}} \right] \quad (1)$$

Where v is lineal piston velocity in $\frac{m}{s}$, r is the crank length in m, l is the crank length in m, θ is the phase shift in rad, ω is the angular velocity in $\frac{rad}{s}$ and t is the time in s. If the angular velocity is positive, the cycle operates as a heat pump. If the angular velocity is negative, the cycle operates as a refrigerator. In the simulation, the angular velocity will always be negative.

The simplified engine's model for the simulation can be seen on **Figure 4** and **Figure 5**. Key components of the engine include the regenerator and the hot and cold heat exchangers, each playing a critical role in the engine's efficiency and overall performance. The regenerator acts as a temporary energy storage unit, recovering heat from the gas as it transitions between the hot and cold zones, thus enhancing the engine's thermal efficiency. Conversely, the heat exchangers facilitate the transfer of heat into and out of the system, crucial for maintaining the temperature gradients essential for the engine's operation.

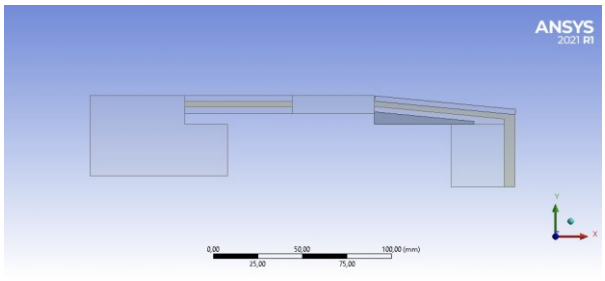

Figure 4. Geometry of the simulation. Design Modeler screenshot.

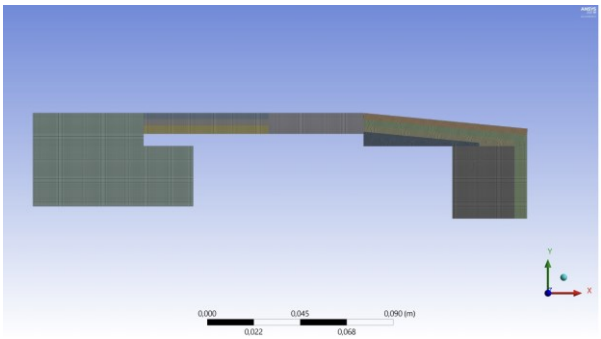

Figure 5. Geometry of the simulation. Mesh screenshot.

The technical specifications of the engine can be seen in the following table. These data have been used for the validation of the results obtained from the simulation.

Table 1. *Main technical specifications of the ZIF-1000 Stirling engine.*

Rotation frequency	1480		rpm
Working gas	helium		
Initial working gas pressure	19		bar
Mean working gas pressure	min 25	max 26	bar
Cooling Heat	16850		W
Power extracted to Air	895		
Liquid Air flow rate	2.11		$\frac{g}{s}$
Cold efficiency	4.8		%
Heat efficiency	91.79		%
Total efficiency	96,59		%
Heater temperature	min 60	max 62	° C
Cooler temperature	min -196	max -193	° C
Displacer	bore 70	stroke 30	mm
Working piston	bore 90	stroke 52	mm
Nominal power	18400	electric	W

Simulation Setup in ANSYS-Fluent

The simulation of the ZIFF-1000 engine in ANSYS-Fluent required a series of preparatory steps to ensure the model accurately reflects the engine's physical and operational characteristics.

After adapting the geometry, the next step is meshing. For the meshing process, the dynamic nature of the engine was considered, particularly the movement of the pistons and the helium gas flow through the various engine components. It is crucial to highlight that in dynamic areas, that is, in the expansion and compression chambers, a rectangular mesh had to be adapted, allowing the use of the *layering* technique for dynamic meshing. A node distance of $\Delta x = 0{,}5\ mm$ was selected. These areas can be seen in the following figures.

Regarding the models used, the energy model and the k-omega SST viscous model have been activated. The rest of the configuration has been left as default.

Regarding the "cell zone conditions," the type of fluid in each zone (helium, air, and water) was specified, and the porous model was activated in the cold, hot exchangers, and the regenerator.

The porosities in the three zones (cold exchanger, hot exchanger, and regenerator) were calculated as follows:

$$\gamma_F = \frac{V_f}{V_T} \tag{2}$$

where γ_F is the porosity of the focus, γ_F is the fluid volume, and V_T is the total volume.

The porosities were determined as follows:

Table 2. *Porosities*

Cold focus exchanger	0,385
Hot focus exchanger	0,205
Regenerator	0,732

As for the boundary conditions, they were adapted so that the simulation includes a constant mass flow rate of water and air. All external walls of the simulation, i.e., those not in contact with a fluid on both sides, are adiabatic. Inlet and conditions for air and water have a temperature of 27 ℃.

Table 3. *Boundary conditions*

Water flow rate	0,357	$\frac{kg}{s}$
Inlet water velocity	0,383512	$\frac{m}{s}$
Outlet water velocity	0,357100	$\frac{m}{s}$
Air flow rate	0,002110	$\frac{kg}{s}$
Inlet air velocity	1,855012	$\frac{m}{s}$
Outlet air velocity	0,002110	$\frac{m}{s}$

Regarding dynamic meshing, the layering method was used, taking advantage of the fact that the mesh in the zones with movement is rectangular, a necessary condition for this method of dynamic meshing. The movement of the piston and displacer is imposed by a UDF (User-Defined Function) that calculates the speed from (1).

To reach the steady-state regime of the simulation more quickly, the initial conditions were divided into two stages: a first phase called common initialization and a second phase called helium pressure initialization. In the first stage, the temperatures of the cold focus walls are also fixed at -223 ℃. Once the air reaches a temperature below -194 ℃, the fixed temperatures of the walls are released to finally achieve the steady state. The initial conditions for the experiment start with helium at a gauge pressure of 4,750,000 Pa, significantly higher than the air and water pressure, which is at atmospheric level (0 Pa). The setup is characterized by an axial velocity of 0 m/s, turbulent kinetic energy set to 1 m^2/s^2, and a specific dissipation rate of 1 s^(-1), with an overall temperature maintained at 300 K.

Residual, relaxation factors and numerical methods were left as default.

Finally, a simulation was launched with $\Delta t = 0{,}00012\ s$ and 10,000-time steps. The restriction of the maximum time step based on mesh size is given by:

$$\Delta t_{max} < \frac{\Delta x_{\max}}{v_{max}} \tag{3}$$

For the case of the simulation, $\Delta x_{\max} = 5 \cdot 10^{-4}\ [m]$ y $v_{max} = 4{,}03 \frac{m}{s}$, therefore $\Delta t_{max} = 1{,}2408 \cdot 10^{-4}\ s$.

Results

In the steady-state regime of our beta Stirling engine simulation for very low temperatures, the validation against the real machine ZIFF-1000 trial was conducted. **Figure 6** indicates the achievement of steady state, which allowed for a direct comparison of simulation outcomes with experimental data. Initial conditions for the simulation were set with water and air mass flow rates at 0.3571 kg/s and 0.00211 kg/s, respectively, both at an entry temperature of 300 K, and helium at an initial pressure of 47.5 bar and temperature of 300 K.

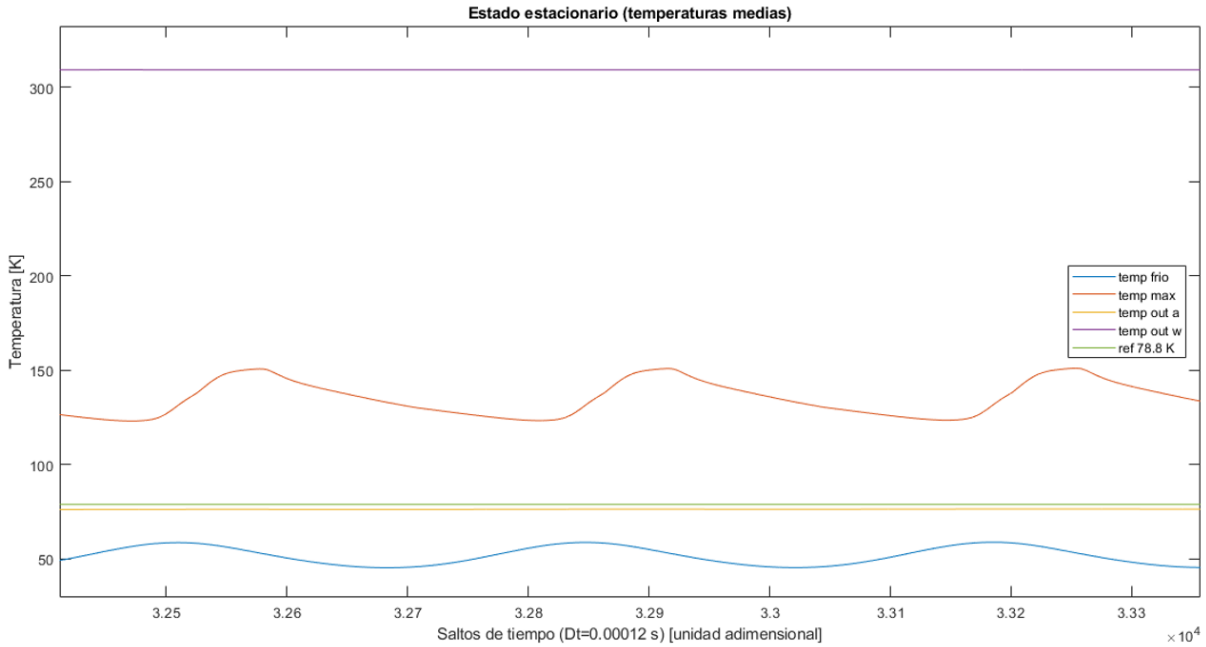

Figure 6. Temperatures distribution of the Stirling engine at the steady state.

Table 4. *Comparison between experimental data and simulations.*

	Experimental data	Simulation
Mean pressure $(\boldsymbol{bar})$	25~26	27,12
Air flow rate $\left(\frac{g}{s}\right)$	2,11	2,11
Cold focus heat $(\boldsymbol{W})$	900	910,31
Hot focus heat $(\boldsymbol{W})$	16850	14008,3

The simulation results, including mean helium pressure, liquid air generation, and cold focus heat, align closely with the trial data, indicating a high degree of accuracy. However, a notable discrepancy exists in the hot focus heat. This discrepancy can be justified by several factors:

- In the real machine trial, the cooling water traverses other hot areas of the machine, unlike in the simulation where it is used solely to cool the Stirling cycle.
- The porous media representing heat exchanger slots and the regenerator are idealized in the simulation, leading to an expected higher engine performance and consequently less heat needing to be cooled for the same level of cooling, as observed in the results.
- The simulation does not account for the heat generated by the friction of moving parts, resulting in less heat to be evacuated by water.

Considering these factors, and comparing the simulation results to the trial data, the simulation within this thesis is deemed coherent with the real experiment outcomes.

Simulation Results Overview

The temperature distribution within the Stirling engine delineates two distinct zones: higher temperatures in the compression chamber and lower temperatures in the expansion chamber, influenced by helium flow and the thermal conductivity of solid copper components. The maximum temperature in the expansion chamber, near 150 K at the

regenerator interface, highlights the cooling limit imposed by this peak temperature on the engine's performance.

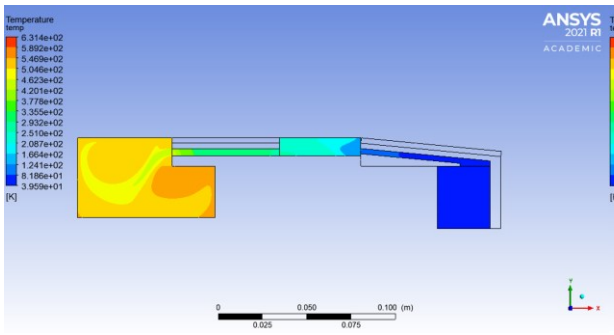

Figure 7. Temperature contour at 0° crankshaft position.

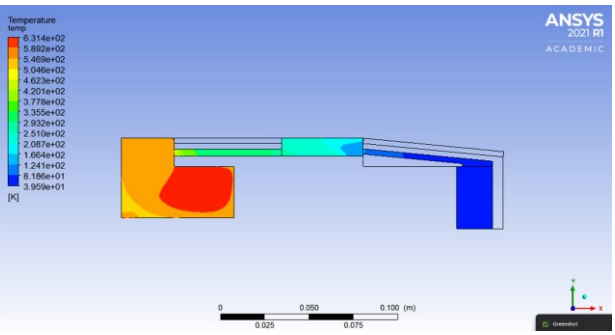

Figure 8. Temperature contour at 90° crankshaft position.

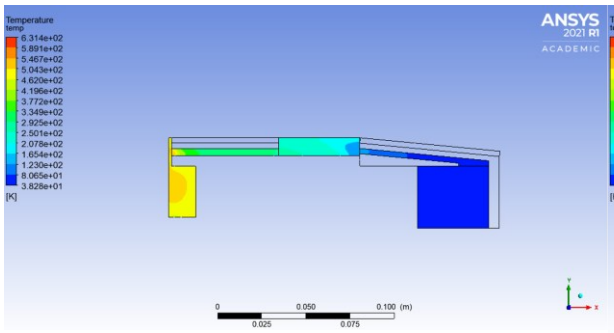

Figure 9. Temperature contour at 180° crankshaft position.

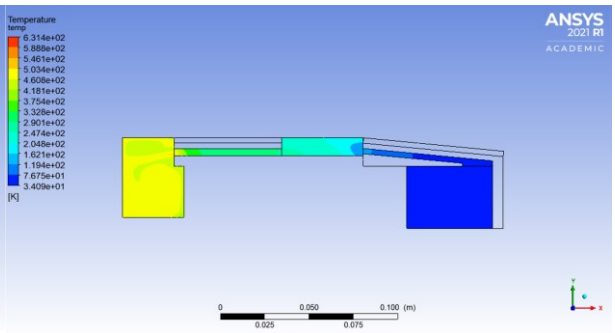

Figure 10. Temperature contour at 270° crankshaft position.

The PV diagram (**Figure 11**) of the Stirling engine displays an oval shape with a closed cycle indicating the system has reached a steady state. This observation confirms the engine's operation within its intended thermodynamic parameters. The closed cycle in the s-T diagram (**Figure 12**) shows that the minimum temperature remains well above 78.8 K, attributed to averaging temperatures across the entire cycle. This method of averaging temperatures across the cycle leads to the expansion chamber's specific temperature values being less distinguishable, emphasizing a strategic decision in how temperature data is presented.

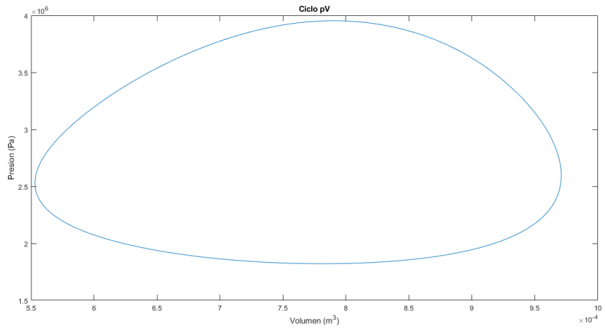

Figure 11. PV diagram of the steady state of the ZIF-1000.

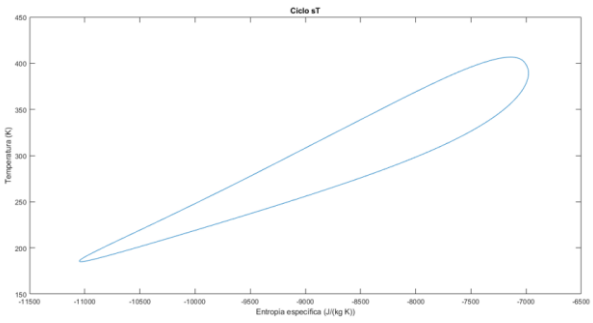

Figure 12. sT diagram of the steady state of the ZIF-1000.

Conclusion and Future Work

This article confirms the coherence between the simulated results and the experimental data of the ZIFF-1000 Stirling engine, particularly in terms of mean working pressure. The simulation demonstrates higher efficiency compared to the actual machine, primarily

evidenced by the differences in hot focus heat. The behavior of the regenerator aligns with expectations from other independent studies, supporting the validity of using constant properties for the working fluid's thermal conductivity, specific heat, and dynamic viscosity.

It has been shown that equivalent heat transfer can be achieved by modifying the fluid properties for simplified analysis. A pseudo-transient regime was effectively employed to expedite the simulation's convergence to a steady state, aligning with the known characteristics of the Stirling engine.

The cryogenic capability of the engine is notably influenced by the temperature rise due to hot helium moving into the expansion chamber, impacting the temperatures of the engine's solid zones.

Future Work

To improve the simulation model's accuracy for Stirling engines under cryogenic conditions, the proposals include developing an advanced User-Defined Function (UDF) for modeling non-equilibrium behavior in porous media, adjusting for volume variations within simulation domains. This enhancement aims to refine heat exchange and fluid dynamics simulations within the engine, especially around gas interactions with porous heat exchangers and regenerators. Additionally, a comprehensive analysis of pressure loss parameters through experimental and simulation studies is suggested to identify accurate correlations for pressure drops across heat exchangers and regenerators, thereby enhancing the model's ability to replicate real-world engine performance, with a focus on minimizing efficiency losses.

References

[1] Robert Stirling. (1816). Regenerator and Hot Air Engines [Patente No. 4081]. Reported by THE ENGINEER. Retrieved from http://hotairengines.org/patents/stirling-patents/THE%20ENGINEER_Stirling's%201816%20patent.pdf.

[2] Hebert, L. (1827). Air Engines [Patent of 1827]. In Galloway, p. 667. Description from Galloway. Retrieved from http://hotairengines.org/patents/stirling-patents/GALLOWAY_Stirling%20engines%201827.pdf.

[3] West, C. (1986). Principles and applications of Stirling engines. Van Nostrand Reinhold.

[4] Buliński, Z., Kabaj, A., Krysiński, T., Szczygieł, I., Stanek, W., Rutczyk, B., ... Gładysz, P. (2019). A Computational Fluid Dynamics analysis of the influence of the regenerator on the performance of the cold Stirling engine at different working conditions. Energy Conversion and Management, 195, 125–138. https://doi.org/10.1016/j.enconman.2019.04.089

[5] Jajcevic, D., Almbauer, R., Schmidt, S., & Karl, G. (2009). Simulation Strategy and Analysis of a Two-Cylinder Two Stroke Engine Using CFD Code Fluent. In Simulation for Innovative Design (pp. 235-246).

[6] Costa Pereira, S. (2014). Numerical characterization study of pressure drop and heat transfer phenomena in woven wire matrix of a Stirling engine regenerator [Tesis de doctorado, Universidad de Mondragón].

[7] Ackermann, R. (1997). Cryogenic Regenerative Heat Exchangers. Plenum Publishing Corporation.

[8] Katooli, M. H., Askari Moghadam, R., & Hajinezhad, A. (2019). Simulation and experimental evaluation of Stirling refrigerator for converting electrical/mechanical energy to cold energy. Energy Conversion and Management, 184, 83–90. https://doi.org/10.1016/j.enconman.2019.01.014

[9] Ahmed, F., Hulin, H., & Khan, A. M. (2019). Numerical modeling and optimization of beta-type Stirling engine. Applied Thermal Engineering, 149, 385–400. https://doi.org/10.1016/j.applthermaleng.2018.12.003